

ANALYSIS AND CONTROL OF FINANCIAL ENGINEERING MODELS

Lakshmi. N. Sridhar

Chemical Engineering Department , University of Puerto Rico, Mayaguez, PR 00681

ABSTRACT

In recent years, high nonlinearities in the dynamics of financial markets have triggered a lot of research in financial engineering to try to deal with fluctuations and develop strategies to control the prices. Bifurcation analysis is a powerful mathematical tool used to deal with the nonlinear dynamics of any process. Several factors must be considered, and multiple objectives must be met simultaneously. Bifurcation analysis and multiobjective nonlinear model predictive control (MNLMP) calculations are performed on two finance models. The MATLAB program MATCONT was used to perform the bifurcation analysis. The MNLMP calculations were performed using the optimization language PYOMO in conjunction with the state-of-the-art global optimization solvers IPOPT and BARON. The bifurcation analysis revealed Hopf bifurcation points branch and limit points in the two models. The Hopf bifurcation points were eliminated using an activation factor involving the tanh function. The branch and limit points were beneficial because they enabled the multiobjective nonlinear model predictive control calculations to converge to the Utopia point in both problems, which is the most beneficial solution. A combination of bifurcation analysis and multiobjective nonlinear model predictive control for financial engineering models is the main contribution of this paper.

KEYWORDS

financial system, bifurcation, optimization, control

1. BACKGROUND

Ma and Chen (2001)[1] studied the topological structure and the global complicated character of a kind of nonlinear finance system. Ma et al (2008)[2] demonstrated the existence of Hopf bifurcations in the financial system on condition of specific combination of parameters. Baur(2012)[3] discussed the connection between financial contagion and the real economy. Chen et al (2013)[4] studied the bifurcation and chaotic behavior of credit risk contagion based on the Fitzhugh-Nagumo system/ Koliai (2016)[5] provided an EVT-pair-copulas approach for financial stress tests. Xu et al (2016)[6] discussed the evolution mechanism of financial system risk.

Huang and co-workers (2017,2018)[7,8] discussed control procedures for synchronization of financial systems. Gong et al (2019)[9] researched chaotic analysis and adaptive synchronization for a class of fractional-order financial systems. Wen and Yang (2019) [10] discussed the complexity evolution of chaotic financial systems based on fractional calculus. Wen et al (2019) [11] explored the dynamic effects of financial factors on oil prices based on a TVP-VAR model. Ma and Li (2020)[12] conducted research on fractional differential equations in the dynamic analysis of a supply chain financial chaotic system. Yang et al (2020)[13] studied the cross-market contagion of economic policy uncertainty and systemic financial risk.

Luo et al (2021)[14] investigated the multiscale financial risk contagion between international stock markets. Akhtaruzzaman et al (2021)[15] studied the financial contagion during the COVID–19 crisis. Shi et al (2022)[16] performed bifurcation analysis and control studies of a fractional-order delay financial system. Wu and Xia(2024)[17] demonstrated the double-well stochastic resonance for a class of three-dimensional financial systems. Zhang et al (2024)[18] discussed the stabilization of a 4D financial system with disturbance and uncertainty by the UDE-based control method. Yan et al (2024) [19] used a type-3 fuzzy logic and Lyapunov approach for dynamic modeling and analysis of financial markets. Stella et al (2024)[20] provided a dynamic model to describe the cascading failures in the global financial system. Wei et al (2024) [21] discussed a procedure to control a new financial risk contagion dynamic model based on finite-time disturbance.

Some of this work involved bifurcation analysis and single-objective optimal control calculation. The main objective of this paper is to perform multiobjective nonlinear model predictive control(MNLMPC) in conjunction with bifurcation analysis for two dynamic financial engineering models. The two models that will be used are those described in Wei et. al. (2024) [28]and Ma e et al (2008)[2]. This paper is organized as follows. First the model equations are presented. The numerical procedures (bifurcation analysis and multiobjective nonlinear model predictive control(MNLMPC) are then described. This is followed by the results and discussion and conclusions.

2. MODEL EQUATIONS

For the first model (Wei et. al. (2024) [28]) the equations are

$$\begin{aligned}\frac{d(xval)}{dt} &= (yval)(zval) - a(xval) + u_1 \\ \frac{d(yval)}{dt} &= (xval)(zval) - b(xval) + u_2 \\ \frac{d(zval)}{dt} &= c(zval) - d(yval) - xval(yval) + u_3\end{aligned}\quad (1)$$

The parameter values are $a=0.5, b=2, c=0.1, d= 4.5$

$xval$ represents the overall risk value of the system that is affected by both external and Internal shocks during the initial stage of any phase, $yval$, is the total risk value of the system arising from contagion effects in the second stage of any phase; and $zval$ denotes the control value for system risk in the third stage of the phase.

For the second model (Ma e et al (2008)[2])

$$\begin{aligned}\frac{d(xval)}{dt} &= zval + (yval - a)xval + u_1 \\ \frac{d(yval)}{dt} &= 1 + b(yval) - (xval)^2 + u_2 \\ \frac{d(zval)}{dt} &= -xval - c(zval) + u_3\end{aligned}\quad (2)$$

The parameter values are $a=4; b=0.125; c=0.5$.

Here x_{val} represents the interest rate, y_{val} is the investment demand, and the price exponent is z_{val} . In both models u_1, u_2, u_3 represent the control parameters.

3. NUMERICAL PROCEDURES

3.1. Bifurcation Analysis

The MATLAB software MATCONT is used to perform the bifurcation calculations. Bifurcation analysis deals with multiple steady-states and limit cycles. Multiple steady states occur because of the existence of branch and limit points. Hopf bifurcation points cause limit cycles. A commonly used MATLAB program that locates limit points, branch points, and Hopf bifurcation points is MATCONT (Dhooge Govearts, and Kuznetsov, 2003[22]; Dhooge Govearts, Kuznetsov, Mestrom and Riet, 2004[23]). This program detects Limit points(LP), branchpoints(BP), and Hopf bifurcation points(H) for an ODE system

$$\frac{dx}{dt} = f(x, \alpha) \quad (3)$$

$x \in R^n$ Let the bifurcation parameter be α Since the gradient is orthogonal to the tangent vector,

The tangent plane at any point $w = [w_1, w_2, w_3, w_4, \dots, w_{n+1}]$ must satisfy

$$Aw = 0 \quad (4)$$

Where A is

$$A = [\partial f / \partial x \quad | \quad \partial f / \partial \alpha] \quad (5)$$

where $\partial f / \partial x$ is the Jacobian matrix. For both limit and branch points, the matrix $[\partial f / \partial x]$ must be singular. The $n+1$ th component of the tangent vector $w_{n+1} = 0$ for a limit point (LP) and for a branch point (BP) the matrix $\begin{bmatrix} A \\ w^T \end{bmatrix}$ must be singular. At a Hopf bifurcation point,

$$\det(2f_x(x, \alpha) @ I_n) = 0 \quad (6)$$

@ indicates the bialternate product while I_n is the n-square identity matrix. Hopf bifurcations cause limit cycles and should be eliminated because limit cycles make optimization and control tasks very difficult. More details can be found in Kuznetsov (1998[24]; 2009[25]) and Govaerts [2000] [26]

3.2. Multiobjective Nonlinear Model Predictive Control(MNLMPC)

Flores Tlacuahuaz et al (2012)[27] developed a multiobjective nonlinear model predictive control (MNLMPC) method that is rigorous and does not involve weighting functions or additional constraints. This procedure is used for performing the MNLMPC calculations Here

$\sum_{t_i=0}^{t_i=t_f} q_j(t_i)$ ($j=12..n$) represents the variables that need to be minimized/maximized simultaneously for a problem involving a set of ODE

$$\frac{dx}{dt} = F(x, u) \quad (7)$$

t_f being the final time value, and n the total number of objective variables and u the control parameter. This MNLMPC procedure first solves the single objective optimal control problem

independently optimizing each of the variables $\sum_{t_i=0}^{t_i=t_f} q_j(t_i)$ individually. The

minimization/maximization of $\sum_{t_i=0}^{t_i=t_f} q_j(t_i)$ will lead to the values q_j^* . Then the optimization problem that will be solved is

$$\begin{aligned} \min & \left(\sum_{j=1}^n \left(\sum_{t_i=0}^{t_i=t_f} q_j(t_i) - q_j^* \right) \right)^2 \\ \text{subject to} & \frac{dx}{dt} = F(x, u); \end{aligned} \quad (8)$$

This will provide the values of u at various times. The first obtained control value of u is implemented and the rest are discarded. This procedure is repeated until the implemented and

the first obtained control values are the same or if the Utopia point where $\left(\sum_{t_i=0}^{t_i=t_f} q_j(t_i) = q_j^* \right)$ for all j is obtained.

Pyomo (Hart et al, 2017)[28] is used for these calculations. Here, the differential equations are converted to a Nonlinear Program (NLP) using the orthogonal collocation method. The NLP is solved using IPOPT (Wächter And Biegler, 2006)[29] and confirmed as a global solution with BARON (Tawarmalani, M. and N. V. Sahinidis 2005)[30].

The steps of the algorithm are as follows

1. Optimize $\sum_{t_i=0}^{t_i=t_f} q_j(t_i)$ and obtain q_j^* at various time intervals t_i . The subscript i is the index for each time step.
2. Minimize $\left(\sum_{j=1}^n \left(\sum_{t_i=0}^{t_i=t_f} q_j(t_i) - q_j^* \right) \right)^2$ and get the control values for various times.
3. Implement the first obtained control values
4. Repeat steps 1 to 3 until there is an insignificant difference between the implemented and the first obtained value of the control variables or if the Utopia point is achieved. The

Utopia point is when $\sum_{t_i=0}^{t_i=t_f} q_j(t_i) = q_j^*$ for all j .

Sridhar (2024a)[31] proved that the MNLMPC calculations to converge to the Utopia solution when the bifurcation analysis revealed the presence of limit and branch points . This was done by imposing the singularity condition on the co-state equation (Upreti, 2013)[32]. If the minimization of q_1 lead to the value q_1^* and the minimization of q_2 lead to the value q_2^* The MNLMPC calculations will minimize the function $(q_1 - q_1^*)^2 + (q_2 - q_2^*)^2$. The multiobjective optimal control problem is

$$\min (q_1 - q_1^*)^2 + (q_2 - q_2^*)^2 \quad \text{subject to} \quad \frac{dx}{dt} = F(x, u) \quad (9)$$

Differentiating the objective function results in

$$\frac{d}{dx_i} ((q_1 - q_1^*)^2 + (q_2 - q_2^*)^2) = 2(q_1 - q_1^*) \frac{d}{dx_i} (q_1 - q_1^*) + 2(q_2 - q_2^*) \frac{d}{dx_i} (q_2 - q_2^*) \quad (10)$$

The Utopia point requires that both $(q_1 - q_1^*)$ and $(q_2 - q_2^*)$ are zero. Hence

$$\frac{d}{dx_i} ((q_1 - q_1^*)^2 + (q_2 - q_2^*)^2) = 0 \quad (11)$$

the optimal control co-state equation (Upreti; 2013) is

$$\frac{d}{dt} (\lambda_i) = - \frac{d}{dx_i} ((q_1 - q_1^*)^2 + (q_2 - q_2^*)^2) - f_x \lambda_i; \quad \lambda_i(t_f) = 0 \quad (12)$$

λ_i is the Lagrangian multiplier. t_f is the final time. The first term in this equation is 0 and hence

$$\frac{d}{dt} (\lambda_i) = -f_x \lambda_i; \lambda_i(t_f) = 0 \quad (13)$$

At a limit or a branch point, for the set of ODE $\frac{dx}{dt} = f(x, u)$ f_x is singular. Hence there are two different vectors-values for $[\lambda_i]$ where $\frac{d}{dt} (\lambda_i) > 0$ and $\frac{d}{dt} (\lambda_i) < 0$. In between there is a vector $[\lambda_i]$ where $\frac{d}{dt} (\lambda_i) = 0$. This coupled with the boundary condition $\lambda_i(t_f) = 0$ will lead to $[\lambda_i] = 0$ This makes the problem an unconstrained optimization problem, and the only solution is the Utopia solution.

Hopf bifurcations cause unwanted oscillatory behavior and limit cycles. The tanh activation function (where a control value u is replaced by $(u \tanh u / \varepsilon)$ is commonly used in neural nets (Dubey et al 2022[33]; Kamalov et al, 2021[34] and Szandała, 2020[35])and optimal control problems(Sridhar 2023[36]) to eliminate spikes in the optimal control profile. Hopf bifurcation points cause oscillatory behavior. Oscillations are similar to spikes, and the results in Sridhar(2024b) demonstrate that the tanh factor also eliminates the Hopf bifurcation by preventing the occurrence of oscillations. Sridhar (2024b)[37] explained with several examples how the activation factor involving the tanh function successfully eliminates the limit cycle causing Hopf bifurcation points. This was because the tanh function increases the time period of the oscillatory behavior, which occurs in the form of a limit cycle caused by Hopf bifurcations.

4. RESULTS AND DISCUSSION

In the first problem, u_1, u_2, u_3 were individually used as bifurcation parameters. When u_1 was the bifurcation parameter, two Hopf bifurcation points, and one branch point were found at $(xval, yval, zval, u_1)$ values of $(0.044, 0.0206, 0.936, 0.0027)$; $(0.044, -0.0206, -0.936, 0.0027)$ and $(0.044, 0.0, 0.0, 0.022)$. The bifurcation diagram is shown in Fig. 1a. The limit cycles for the two Hopf bifurcations are shown in Figures 1b and 1c. When the bifurcation parameter was modified to $u_1 \tanh(u_1)/3800$, the Hopf bifurcation disappears. This is shown in Fig. 1d.

When u_2 was the bifurcation parameter, a Hopf bifurcation point and a limit point were found at $(xval, yval, zval, u_2)$ values of $(0.037710, 0.020384, 0.924982, 0.005887)$ and $(0.014702, 0.012760, 0.576079, 0.017051)$ (Fig. 2a). The limit cycle produced by this Hopf bifurcation point is shown in Fig. 2b. When the bifurcation parameter was modified to $u_2 \tanh(u_2)/0.005$ the Hopf bifurcation point disappears. Still, the limit point occurs at $(0.014702, 0.012760, 0.576090, 0.009233)$. This is shown in Fig. 2c.

When u_3 was the bifurcation parameter, a Hopf bifurcation point was found at $(xval, yval, zval, u_3)$ values of $(0.0938, 0.0469, 1.0, 0.11554)$ (Fig. 3a). A limit cycle is caused by this Hopf bifurcation point (Fig. 3 b). When the bifurcation parameter was modified to $u_3 \tanh(u_3)/100$ the Hopf bifurcation point disappears (Fig. 3c).

When the MNLMPCC calculations were performed $\sum_{t_i=0}^{t_i=t_f} xval_j(t_i), \sum_{t_i=0}^{t_i=t_f} yval_j(t_i), \sum_{t_i=0}^{t_i=t_f} zval_j(t_i)$ were minimized individually each leading to a value of 0 and The overall optimal control problem will involve the minimization of $(\sum_{t_i=0}^{t_i=t_f} xval_j(t_i))^2 + (\sum_{t_i=0}^{t_i=t_f} yval_j(t_i))^2 + (\sum_{t_i=0}^{t_i=t_f} zval_j(t_i))^2$ was minimized subject to the equations governing the model. This led to a value of zero (the Utopia solution). The first of the control variables is implemented, and the rest are discarded. The process is repeated until the difference between the first and second values of the control variables are the same. This MNLMPCC control values of u_1, u_2, u_3 obtained were (1.7435, 2.252, 6.254). The various MNLMPCC profiles are shown in Figs 4a and 4b. . The obtained control profile of s exhibited noise (Fig.4 b). This was remedied using the Savitzky-Golay Filter. The smoothed-out version of this profile is shown in Fig.4c.

In the second problem, u_1, u_2, u_3 were individually used as bifurcation parameters. When u_1 was the bifurcation parameter, a Hopf bifurcation point, and a limit point were found at $(xval, yval, zval, u_1)$ values of $(1.225987, 4.024362, -2.451975, 2.422107)$ and $(0.763763, -3.333332, -1.527525, 7.128451)$

(Fig. 5a) The limit cycle generated by this Hopf bifurcation point is shown in Fig. 5 b. When the bifurcation parameter was modified to $u_1 \tanh(u_1)/0.1$, the Hopf bifurcation disappears but two limit points are obtained at label $(0.763763, -3.333331, -1.527526, 0.958583)$ and $(0.763763, -3.333331, -1.527526, -0.958583)$. This is shown in Fig. 5c. There were no bifurcations when u_2 was the bifurcation parameter.

When u_3 was the bifurcation parameter, a Hopf bifurcation point and a limit point was found at $(xval, yval, zval, u_3)$ values of $(1.225 \ 4.024-0.0298 \ 1.211)$ and $(0.7637 \ -3.333 \ 5.600 \ 3.564)$. This is shown in Fig. 6a. The Hopf bifurcation point generates a limit cycle that is shown in Fig. 6b. When the bifurcation parameter was modified to $u_3 \tanh(u_3)/0.1$ the Hopf bifurcation point disappears (Fig. 6c). The limit point still occurs at $(0.763-3.33 \ 5.60 \ 0.634)$ (Fig. 6c).

When the MNL MPC calculations were performed $\sum_{t_i=0}^{t_i=t_f} xval_j(t_i), \sum_{t_i=0}^{t_i=t_f} yval_j(t_i), \sum_{t_i=0}^{t_i=t_f} zval_j(t_i)$ were minimized individually each leading to a value of 0 and the overall optimal control problem will involve the minimization of $(\sum_{t_i=0}^{t_i=t_f} xval_j(t_i))^2 + (\sum_{t_i=0}^{t_i=t_f} yval_j(t_i))^2 + (\sum_{t_i=0}^{t_i=t_f} zval_j(t_i))^2$ was minimized subject to the equations governing the model. This led to a value of zero (the Utopia solution). The first of the control variables is implemented, and the rest are discarded. The process is repeated until the difference between the first and second values of the control variables is the same. This MNL MPC control values of u_1, u_2, u_3 obtained were $(3.03669 \ 6.94238 \ 4.02158)$. The various MNL MPC profiles are shown in Figs 7a and 7b. The obtained control profile of s exhibited noise (Fig. 7b). This was remedied using the Savitzky-Golay Filter. The smoothed-out version of this profile is shown in Fig. 7c.

In both cases, the MNL MPC calculations converged to the Utopia solution, Sridhar (2024a)[31], which showed that the presence of a limit or branch point enables the MNL MPC calculations to reach the best possible (Utopia) solution. Both problems exhibited limit cycles causing Hopf bifurcation points, which were successfully eliminated using an activation factor involving the tanh function, confirming the analysis of Sridhar (2024b)[37]. Sridhar(2024b)[37] explained with several examples how the activation factor involving the tanh function successfully eliminates the limit cycle causing Hopf bifurcation points by increasing the period of the oscillatory behavior, which occurs in the form of a limit cycle.

5. CONCLUSIONS

Multiobjective nonlinear model predictive control calculations were performed along with bifurcation analysis on two dynamic financial engineering models. The bifurcation analysis revealed the existence of Hopf bifurcation points, limit points, and branch points. The Hopf bifurcation points cause unwanted limit cycles and were eliminated using a tanh activation factor. The limit and branch points (which produced multiple steady-state solutions originating from a singular point) are very beneficial as they caused the multiobjective nonlinear model predictive calculations to converge to the Utopia point (the best possible solution) in both models. A combination of bifurcation analysis and multiobjective nonlinear model predictive control for financial engineering models is the main contribution of this paper.

DATA AVAILABILITY STATEMENT

All data used is presented in the paper

CONFLICT OF INTEREST

The author, Dr. Lakshmi N Sridhar has no conflict of interest.

ACKNOWLEDGEMENT

Dr. Sridhar thanks Dr. Carlos Ramirez and Dr. Suleiman for encouraging him to write single-author papers.

REFERENCES

- [1] Ma, J. H., and Y. S. Chen, Study for the bifurcation topological structure and the global complicated character of a kind of nonlinear finance system (I), *Applied Mathematics and Mechanics*, 2001, 22(11): 1240{1251.
- [2] MA, J., CUI, Y. & LIU, L. Hopf bifurcation and chaos of financial system on condition of specific combination of parameters*. *J Syst Sci Complex* **21**, 250–259 (2008).
- [3] Baur, D.G. Financial contagion and the real economy. *J. Bank. Financ.* **2012**, 36, 2680–2698.
- [4] Chen, T.Q.; He, J.M.; Wang, J.N. Bifurcation and chaotic behavior of credit risk contagion based on Fitzhugh-Nagumo system. *Int. J. Bifurc. Chaos* **2013**, 23, 1350117.
- [5] Koliai, L. Extreme risk modeling: An EVT–pair-copulas approach for financial stress tests. *J. Bank. Financ.* **2016**, 70, 1–22.
- [6] Xu, Y.; Xie, C.; Wang, Y. Evolution mechanism of financial system risk. *Stat. Decis.* **2016**, 1, 172–175.
- [7] Huang, C.; Cao, J. Active control strategy for synchronization and anti-synchronization of a fractional chaotic financial system. *Phys. A* **2017**, 473, 262–275.
- [8] Huang, C.; Cai, L.; Cao, J. Linear control for synchronization of a fractional-order time-delayed chaotic financial system. *Chaos Solitons Fractals* **2018**, 113, 326–332.
- [9] Gong, X.L.; Liu, X.H.; Xiong, X. Chaotic analysis and adaptive synchronization for a class of fractional order financial system. *Phys. A* **2019**, 522, 33–42.
- [10] Wen, C.; Yang, J. Complexity evolution of chaotic financial systems based on fractional calculus. *Chaos Solitons Fractals* **2019**, 128,242–251.
- [11] Wen, F.; Zhang, M.; Deng, M.; Zhao, Y.; Jian, O. Exploring the dynamic effects of financial factors on oil prices based on a TVP-VAR model. *Phys. A* **2019**, 532, 121881.
- [12] Ma, Y.; Li, W. Application and research of fractional differential equations in dynamic analysis of supply chain financial chaotic system. *Chaos Solitons Fractals* **2020**, 130, 109417
- [13] Yang, Z.H.; Chen, L.X.; Chen, Y.T. Cross-market contagion of economic policy uncertainty and systemic financial risk: A nonlinear network connectedness analysis. *Econ. Res. J.* **2020**, 1, 65–81.
- [14] Luo, C.Q.; Liu, L.; Wang, D. Multiscale financial risk contagion between international stock markets: Evidence from EMD-Copula-CoVaR analysis. *N. Am. J. Econ. Financ.* **2021**, 58, 101512.
- [15] Akhtaruzzaman, M.; Boubaker, S.; Sensoy, A. Financial contagion during COVID–19 crisis. *Financ. Res. Lett.* **2021**, 38, 101604.
- [16] Shi, J.; He, K.; Fang, H. Chaos, Hopf bifurcation and control of a fractional-order delay financial system. *Math. Comput. Simul.* **2022**, 194, 348–364.
- [17] Wu, J.; Xia, L. Double well stochastic resonance for a class of three-dimensional financial systems. *Chaos Solitons Fractals* **2024**, 181, 114632.
- [18] Zhang, S.; Zhu, X.; Liu, C. Stabilization of a 4D financial system with disturbance and uncertainty by UDE-based control method. *J. Frankl. Inst.* **2024**, 361, 106897.
- [19] Yan, S.R.; Mohammadzadeh, A.; Ghaderpour, E. Type-3 fuzzy logic and Lyapunov approach for dynamic modeling and analysis of financial markets. *Heliyon* **2024**, 10, e33730.
- [20] Stella, L.; Bauso, D.; Blanchini, F.; Colaneri, P. Cascading failures in the global financial system: A dynamical model. *Oper. Res. Lett.* **2024**, 55, 107122.
- [21] Wei, Y.; Xie, C.; Qing, X.; Xu, Y. Control of a New Financial Risk Contagion Dynamic Model Based on Finite-Time Disturbance. *Entropy* **2024**, 26, 999.
- [22] Dhooge, A., Govaerts, W., and Kuznetsov, A. Y., MATCONT: “A Matlab package for numerical bifurcation analysis of ODEs”, *ACM transactions on Mathematical software* 29(2) pp. 141-164, 2003.
- [23] Dhooge, A., W. Govaerts; Y. A. Kuznetsov, W. Mestrom, and A. M. Riet , “CL_MATCONT”; *A continuation toolbox in Matlab*, 2004.
- [24] Kuznetsov, Y.A. “Elementsofappliedbifurcation theory” .*Springer*, NY, 1998.
- [25] Kuznetsov, Y.A.(2009).”Fivelecturesonnumericalbifurcationanalysis” ,*UtrechtUniversity,NL.*, 2009.

- [26] Govaerts, w. J. F., “Numerical Methods for Bifurcations of Dynamical Equilibria”, *SIAM*, 2000.
- [27] Flores-Tlacuahuac, A. Pilar Morales and Martin Rivalal Toledo; “Multiobjective Nonlinear model predictive control of a class of chemical reactors” *.I & EC research*; 5891-5899, 2012.
- [28] Hart, William E., Carl D. Laird, Jean-Paul Watson, David L. Woodruff, Gabriel A. Hackebeil, Bethany L. Nicholson, and John D. Sirola. “Pyomo – Optimization Modeling in Python” Second Edition. Vol. 67.
- [29] Wächter, A., Biegler, L. “On the implementation of an interior-point filter line-search algorithm for large-scale nonlinear programming”. *Math. Program.* **106**, 25–57 (2006). <https://doi.org/10.1007/s10107-004-0559-y>
- [30] Tawarmalani, M. and N. V. Sahinidis, “A polyhedral branch-and-cut approach to global optimization”, *Mathematical Programming*, 103(2), 225-249, 2005
- [31] Sridhar LN. Coupling Bifurcation Analysis and Multiobjective Nonlinear Model Predictive Control. *Austin Chem Eng.* 2024a; 10(3): 1107.
- [32] Upreti, Simant Ranjan; *Optimal control for chemical engineers.* Taylor and Francis; 2013
- [33] Dubey S. R. Singh, S. K. & Chaudhuri B. B. 2022 Activation functions in deep learning: A comprehensive survey and benchmark. *Neurocomputing*, 503, 92-108. <https://doi.org/10.1016/j.neucom.2022.06.111>
- [34] Kamalov A. F. Nazir M. Safaraliev A. K. Cherukuri and R. Zgheib 2021, "Comparative analysis of activation functions in neural networks," *2021 28th IEEE International Conference on Electronics, Circuits, and Systems (ICECS)*, Dubai, United Arab Emirates, , pp. 1-6, doi:10.1109/ICECS53924.2021.9665646.
- [35] Szandała, T. 2020, Review and Comparison of Commonly Used Activation Functions for Deep Neural Networks. *ArXiv*. <https://doi.org/10.1007/978-981-15-5495-7>
- [36] Sridhar. L. N. 2023 Bifurcation Analysis and Optimal Control of the Tumor Macrophage Interactions. *Biomed J Sci & Tech Res* 53(5). BJSTR. MS.ID.008470.**DOI:** 10.26717/BJSTR.2023.53.008470
- [37] Sridhar LN. Elimination of oscillation causing Hopf bifurcations in engineering problems. *Journal of Applied Math.* 2024b; 2(4): 1826.

APPENDIX

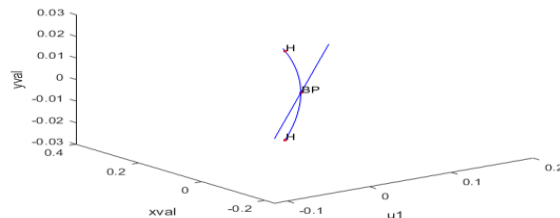


Fig. 1a

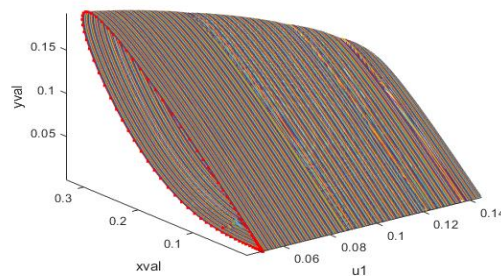


Fig. 1b

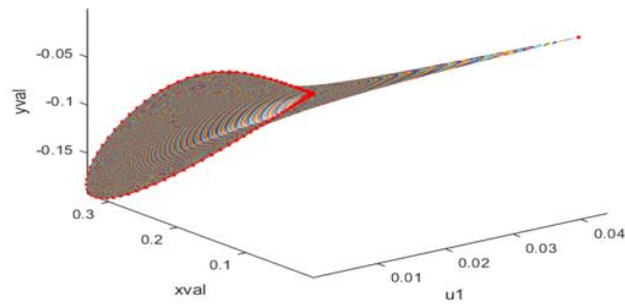
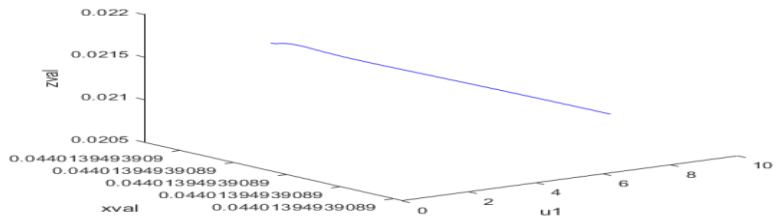


Fig. 1c



Fi. 1d

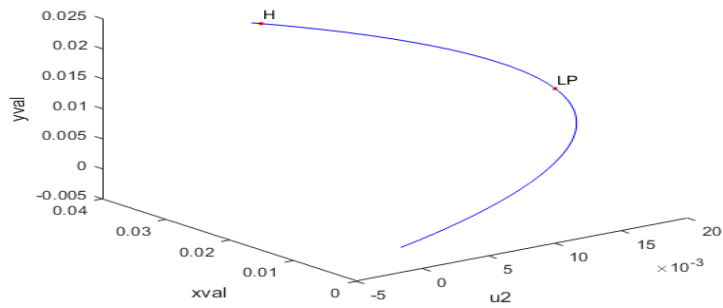


Fig. 2a

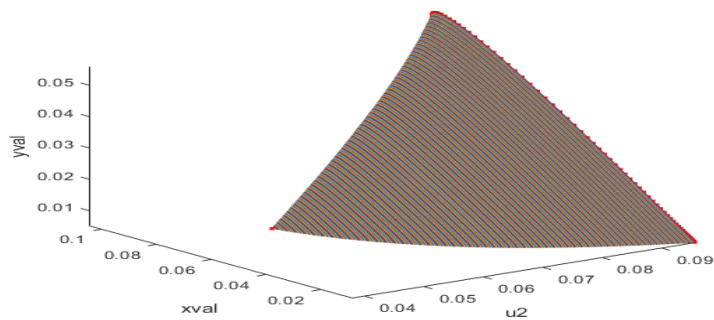


Fig. 2 b

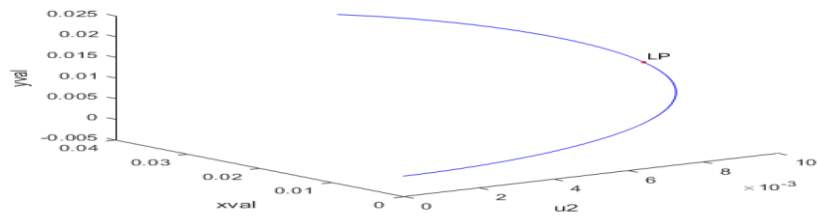


Fig. 2c

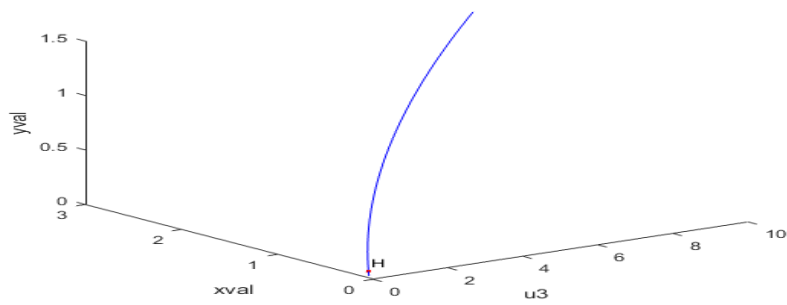


Fig. 3a

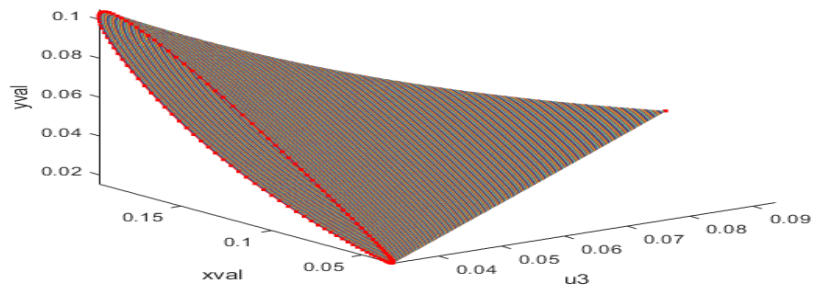


Fig. 3b

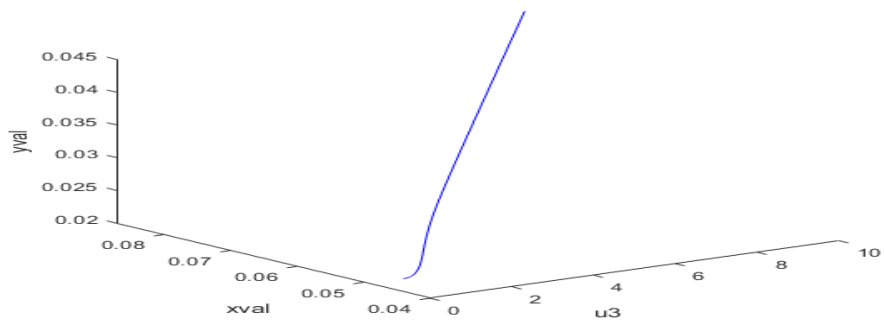


Fig. 3c

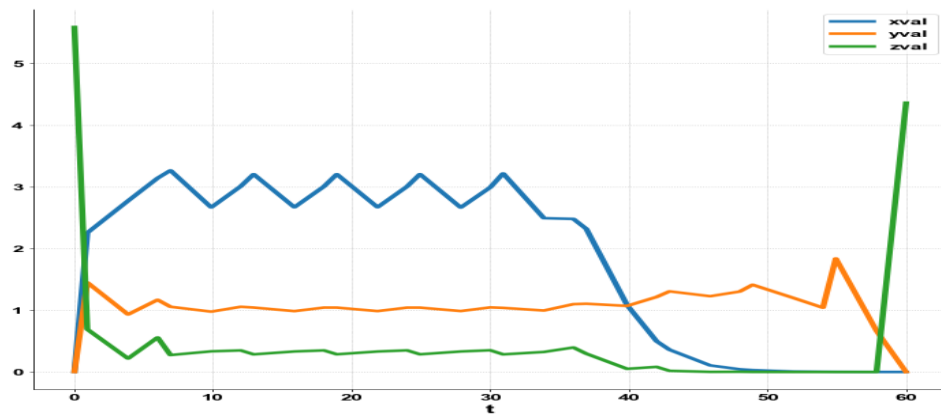


Fig. 4a

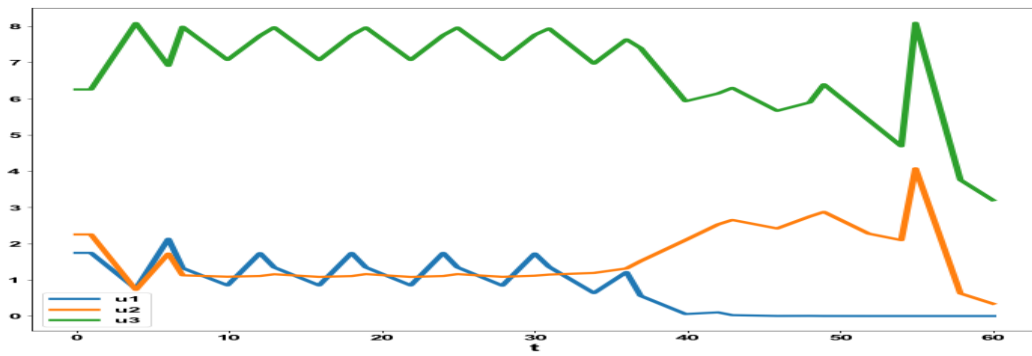


Fig. 4b

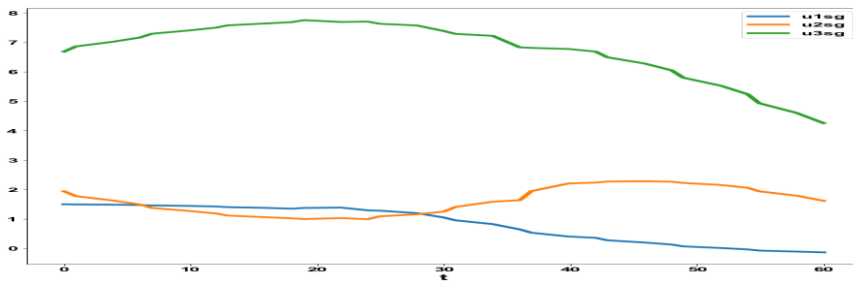


Fig. 4c

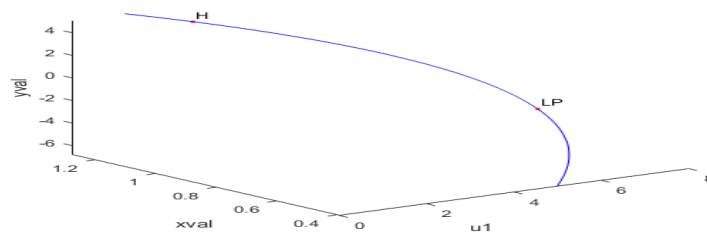


Fig. 5a

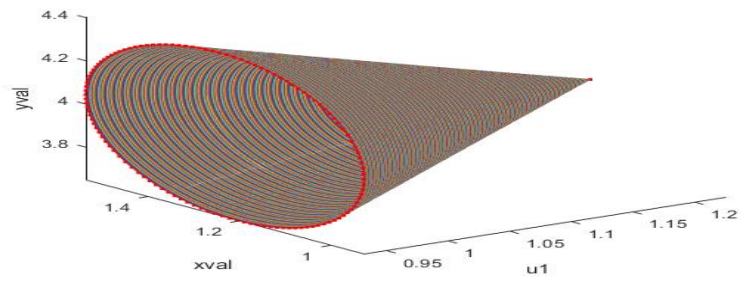


Fig. 5b

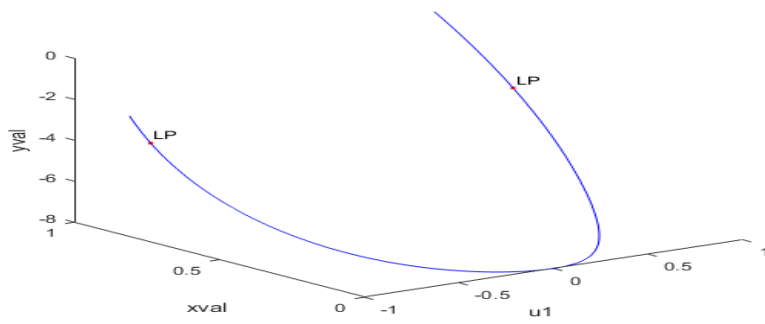


Fig. 5c

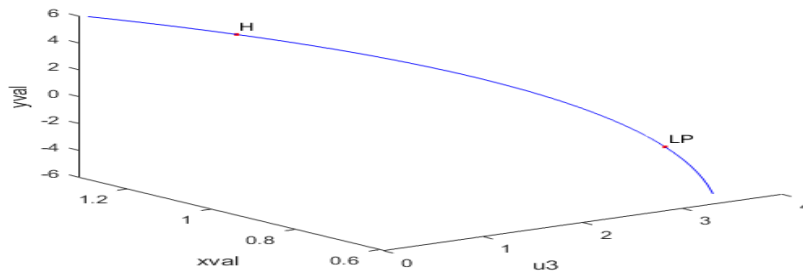


Fig. 6a

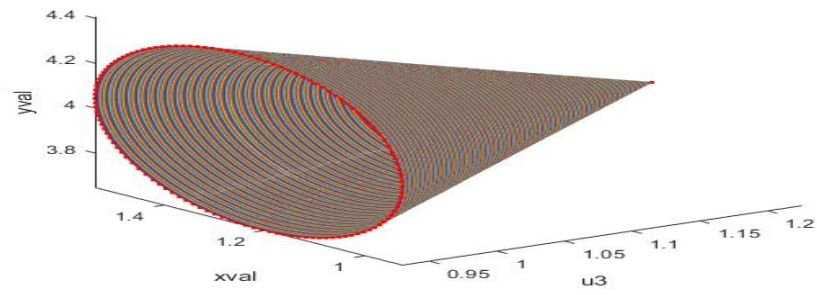


Fig. 6 b

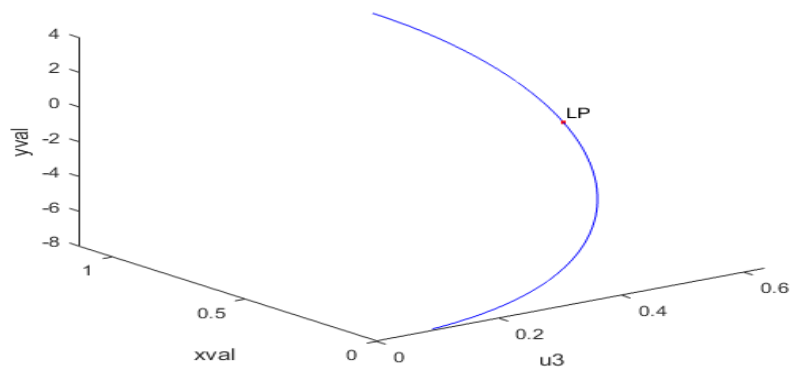


Fig. 6c

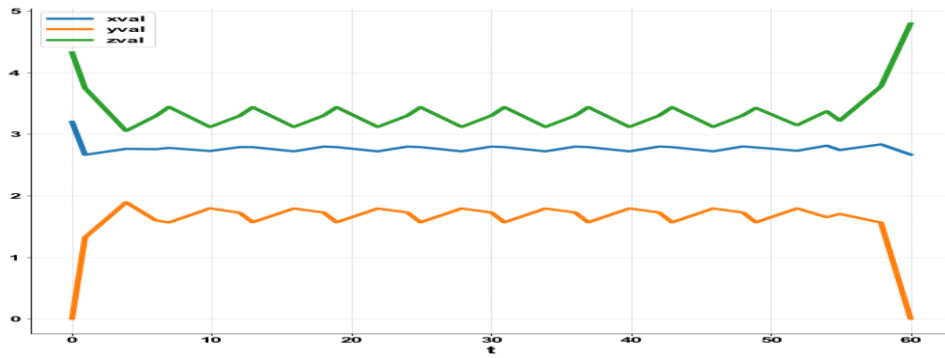


Fig. 7a

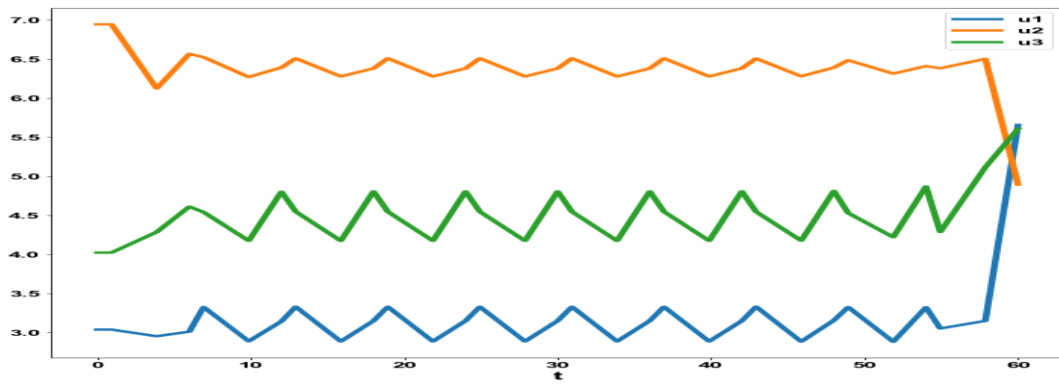


Fig. 7b

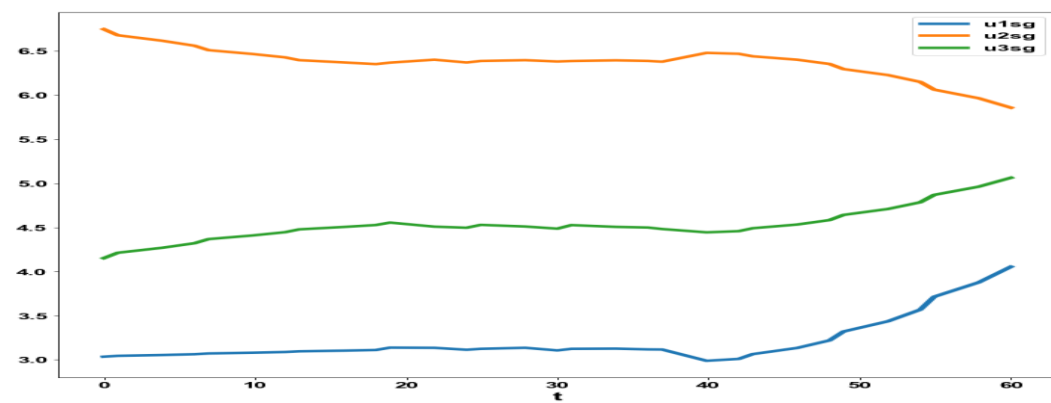


Fig. 7c